

An Exploratory Study of Ice Nucleation by Soot Aerosols

PAUL J. DEMOTT

Department of Atmospheric Science, Colorado State University, Fort Collins, Colorado

9 May 1989 and 30 May 1990

ABSTRACT

The activities of nearly monodisperse soot particles as ice nuclei at temperatures below -20°C were examined in a short series of experiments. A continuous slow expansion cloud chamber was used to cause cloud formation and growth on soot during simulations of adiabatic cooling by expansion. Soot was generated using an acetylene burner operating near the sooting limit. Activity as ice nuclei was measured as clouds cooled to the apparent homogeneous-freezing temperatures of the cloud droplets. Immersion-freezing nucleation appears to be a particularly dominant heterogeneous mode for these particles. The preliminary results suggest that activity by immersion-freezing increases with particle size.

1. Introduction

Carbonaceous soot is a common atmospheric aerosol, and water and ice nucleation are important scavenging processes for such aerosols. Descriptions of the CCN and ice nucleating activity of soot particles are important to the general understanding of man's influence on clouds and precipitation and are especially relevant to the "nuclear winter" hypothesis (National Research Council 1985). Although certain carbonaceous aerosols can function as CCN (Hallett et al. 1989; Hagen et al. 1989), they typically have no ice nucleation activity at temperatures warmer than -15°C (Hallett et al. 1986). At colder temperatures soot particles may act as ice nuclei.

The preliminary studies reported here utilized the dynamic (controlled expansion) cloud chamber at Colorado State University to study the nucleation of ice by carbonaceous soot. Clouds were formed, using the soot as CCN, at cold temperatures ($< -20^{\circ}\text{C}$) so that ice nucleation activity could be observed during continued cooling of cloud droplets to near -40°C .

2. Experimental methods

a. Colorado State University dynamic cloud chamber

The CSU dynamic cloud chamber has been described in some detail by DeMott and Rogers (1990), and DeMott (1988). The chamber consists of a 1.2 m^3 test volume inside a perforated (with small holes) cylindrical copper chamber; wall temperature effects are minimized by circulating temperature controlled

fluid through copper tubing which is soldered to the wall. The copper cylinder is enclosed by a thermally insulated stainless steel pressure vessel of 2 m^3 volume. This volume is evacuated to simulate adiabatic cooling. The temperature of the copper cylinder is controlled to match the adiabatic expansion cooling of the air. Evacuation control, temperature control, and data acquisition are done by microcomputer. Data are recorded at 15 s intervals. Pressure and temperature control are based on equations for dry and moist adiabatic expansion. Air temperature, pressure, humidity, cloud droplet sizes and concentrations, and ice crystals numbers settling from the volume are measured in time.

Temperature is measured continuously using an array of ten copper-Constantan thermocouples (0.508 mm wire) located on the inner liner and two faster response (0.0254 mm wire) thermocouples located 25 cm into the air volume from the inner wall. Typical air temperature uncertainty is 0.2° to 0.3°C . This estimate is based on considering the equilibrium temperatures of stationary wetted or ice surfaces of the same size as the thermocouples. In most cases, the error will be such that the temperature is colder than measured because the thermocouples will be in a condensing environment. A large temperature change may be measured when a water film freezes on the thermocouples, but this increase will be very transient and it has never been detected with the current data system sampling rates. In any case, this should occur once during an experiment (excepting collisions by cloud droplets), after which the measured temperature will be the temperature of the ice surface. Confidence in the relatively small average uncertainty in temperature is given by the measurements taken during the experiments presented in this paper. Figure 1 shows air temperatures at positions lower (T1) and higher (T2) in

Corresponding author address: Dr. Paul DeMott, Department of Atmospheric Sciences, Colorado State University, Fort Collins, CO 80523.

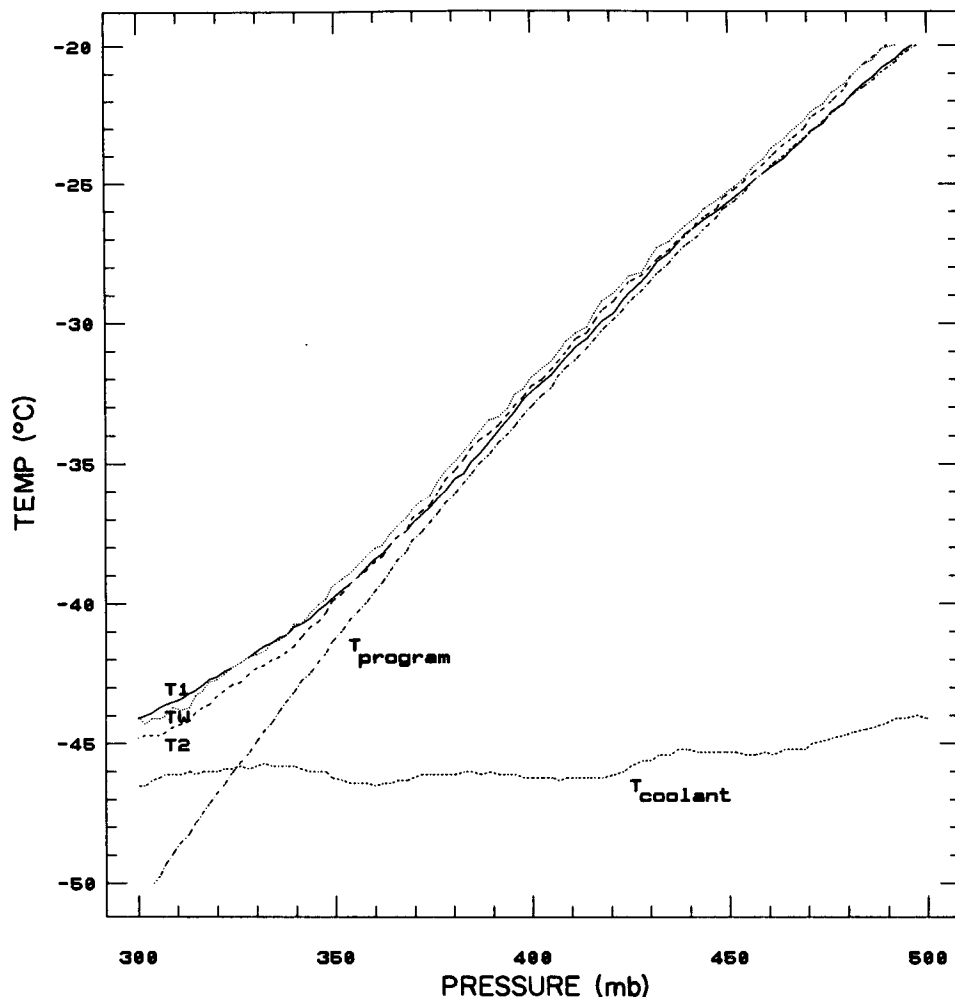


FIG. 1. Temperatures measured versus pressure during a cloud chamber expansion test. Included are air temperature measured in the lower (T1) and upper (T2) regions of the chamber, average wall temperature (TW), coolant source temperature, and the programmed temperature profile. Simulated ascent rate was 2.5 m s^{-1} .

the chamber volume, the average wall temperature (TW), and the coolant source temperature measured as a function of decreasing pressure during a segment of a particular experiment. Also shown is the temperature profile programmed. The simulated ascent rate was 2.5 m s^{-1} in this experiment, so the cooling rate was approximately 1°C min^{-1} while cloud was present (below -24°C). It can be seen that the various temperatures agree within about $\pm 0.4^\circ\text{C}$ of each other over a range of temperatures to nearly -38°C . Larger deviations occur when cloud forms, and below -38°C , when the capacity of the coolant source to keep the walls in step with expansion cooling becomes limited. Most of the important data in this study occurs between -20° and -38°C . Confidence in the accuracy of the air temperature measurement is also given by the agreement of the average wall temperature to within a few tenths of a degree of the air temperatures over the

entire temperature range. The wall thermocouples are epoxied into the outer surface of the inner chamber liner and should never be exposed to condensation.

Pressure is measured with a strain gauge type transducer. Sensitivity is 0.5 mb at room pressure ($\sim 850 \text{ mb}$). Humidity is measured with two optical condensation-type dewpoint hygrometers.

Cloud droplet sizes and concentrations are measured with a Particle Measuring Systems (PMS) FSSP-100. A special sampling system is used to draw cloud from within the chamber through the FSSP laser-optics. The droplet stream is mechanically centered in the optical depth of field. This circumvents some of the measurement problems associated with these instruments when they sample the free stream from aircraft (Dye and Baumgardner 1984; Baumgardner et al. 1985; Copper 1988). There are unavoidable inherent sizing uncertainties for all FSSP probes which particularly occur

in the 1 to 10 μm range of particle sizes due to the behavior of the Mie scattering function there (Pinnick and Auvermann 1979). Multiple Mie peaks for droplets below 10 μm can lead to uncertainties as large as a factor of 2 to 3 in diameter.

Ice crystals are detected by extinction in a laser-based detection device (DeMott and Rogers 1990). Ice crystals settle through a small hole at the base of the liner enclosing the cloud volume and are drawn into the counter inlet. Experiments have shown that the technique responds to cloud droplets, ice particles, and electronic noise. A threshold circuit is used to discriminate against both noise and small cloud droplets. Cloud droplets rarely reach sizes larger than 20 to 25 μm before settling out of the chamber, and ice crystals almost always achieve these sizes before settling out. The threshold is thus adjusted to discriminate against droplets. The largest droplets in the experiments described here were 15 μm , so it is highly unlikely that cloud droplets were mistaken for ice particles. Cloud experiments in the absence of heterogeneous ice nuclei support this conclusion. Calibration of the ice particle counts was made versus "ground truth" collections onto microscope slides. From numerous calibrations, it was found that the standard deviation in ice particle counts was about 30% of the total, independent of temperature or ice crystal habit. The total ice crystal number settled from the chamber was determined by multiplying the ice particle count by the ratio of liner bottom surface area to the sample hole area.

A slight measurement lag occurs because crystals must grow and settle into the ice particle detector. "Instantaneous" pulse nucleation tests using liquid CO_2 and dry ice have shown a nearly Gaussian response peaking 45 to 75 s after nucleation, depending on temperature and pressure (which affect crystal growth rate and fall velocity) when cloud is present. The typical 1 minute lag represents a 1°C error in the temperature attributed to a given ice crystal signal for a 2.5 m s^{-1} ascent rate simulation. It is important to account for this factor for ascent rates of this magnitude or greater. The mathematical procedure used to "back" (deconvolute) the ice crystal signal to be a true nucleation signal is detailed in DeMott and Rogers (1990). Based on that study, the uncertainty associated with the procedure is equivalent to a 0.25°C error in the temperature attributed to a given ice signal for a 2.5 m s^{-1} ascent simulation and 0.50°C for a 5.0 m s^{-1} ascent. These were the two rates used in this study.

Initial conditions for these experiments used ambient temperature ($+20^\circ\text{C}$) and pressure (840 mb) air with a dewpoint of near -16°C and background chamber particle concentrations $<0.1 \text{ cm}^{-3}$, as measured by a condensation nucleus (CN) counter. The lifting condensation level for these conditions occurs at 485 mb, -22.5°C . These are representative of some altocumulus or cirrus cloud conditions, although the choice was simply one of being conveniently at a temperature

where some ice formation could be expected. This is because the experiments were not intended to be simulations of particular atmospheric clouds, but mechanistic studies of ice formation.

b. Soot generation

A schematic of the particle generation system for producing soot aerosols is shown in Fig. 2. Soot particles were generated using a simple oxygen-deficient acetylene burner operated near the sooting limit. The generator is similar to that of Sinclair (1986). Acetylene flow was set the same in all cases. An electrostatic classifier was used to extract nominal monodisperse sizes of 0.08 and 0.15 μm from the polydisperse sample. Based on Cleary et al. (1988), it might be expected that the actual mean volume diameter of the soot was smaller, but only by less than 30%, than the sizes inferred from electrical mobility. Cleary et al. found the discrepancy to increase with larger carbonaceous particle sizes. Scanning electron microscopy checks of the monodisperse particles, collected on nucleopore filters, indicated reasonably uniform particle sizes classified. A range of actual diameters between 0.07 and 0.09 μm were found for the 0.08 μm mobility diameter particles, while the particles classified as 0.15 μm diameter by mobility were actually 0.10 to 0.12 μm diameter. Physically the particles appeared as aggregate "blobs," as opposed to chains.

Immediately after generation, aerosols were passed through a radioactive neutralizer, collected in 12 L electrically conducting plastic bags, and diluted with -30°C dewpoint, particle-free air. Particle concentrations were measured with the CN counter. Samples were vented into the cloud chamber by utilizing the pressure difference between the bag and the chamber at the time of injection. A small mixing fan inside the chamber was used during injection to assure rapid dispersion throughout the chamber volume.

c. Experiment design

Ultimately, it is desired to isolate and quantify the various means by which soot aerosols can initiate the

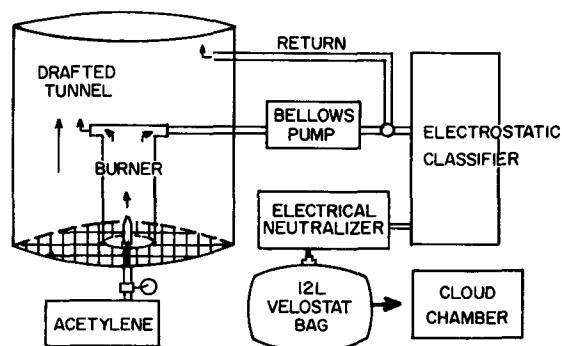


FIG. 2. Schematic of the soot generation and sampling system.

formation of ice for different atmospheric conditions. These preliminary experiments cover only parts of the ranges of temperature and vapor concentration of interest. Also, due to the specific experimental design and the conditions simulated, primarily the condensation and immersion-freezing ice nucleation modes were investigated.

Experiments were purposely set up to cause a large fraction of the soot aerosols to become encapsulated in cloud droplets. Since soot bears no resemblance structurally to known heterogeneous ice nucleants, it was expected that immersion-freezing nucleation would be a predominant ice nucleation mode. This is based on the known influence of insoluble particles (of any chemistry) on the freezing of supercooled water droplets as temperatures approach the supercooling limit of pure water (i.e., Pruppacher and Neiberger 1963). Soot aerosols were injected into nearly particle free air at 0°C during continuous expansions, such that the soot particles were the only particles available as CCN. Clouds formed on these aerosols near -22°C. Little ice nucleation activity was detected at warmer temperatures. Ice nucleation was observed as the air and cloud droplets continued to cool during expansion to -40°C.

For particles acting as CCN, ice nucleation should proceed by condensation-freezing at cloud point and primarily by immersion freezing nucleation upon further cooling of drops. Soot that remains as interstitial particles can take the form of unactivated haze particles whose freezing point is depressed or may act by the additional ice nucleation mechanisms of contact-freezing and deposition nucleation, as defined by Vali (1985). The number of particles injected was adjusted to be approximately the same in each experiment ($\sim 400 \text{ cm}^{-3}$). Simulated ascent rate was 2.5 or 5.0 m s^{-1} in order to vary the supersaturation at cloud point and the cooling rate in cloud.

Although a determination of the CCN activity (versus supersaturation) of the soot aerosols was not required to quantify their immersion-freezing nucleation activity, since droplet concentrations nucleated in any expansion are measured, application of the results to real atmospheric situations does require this knowledge. This information was not rigorously obtained. The continuous flow thermal gradient diffusion chamber technique is an appropriate method for obtaining this information, but was not available for this study. Instead, the microphysical adiabatic cloud model of Young (1974, 1977) was used to estimate the peak supersaturation occurring at thermodynamic cloud point during the cloud chamber expansions. Monodisperse soluble CCN activate at one critical supersaturation, but varying fractions of the monodisperse soot nucleated cloud droplets at different expansion rates (different water supersaturations). This may be due to the condensation of varying quantities of soluble matter on similar sized particles following combustion. The

monodisperse soot was therefore treated as a polydisperse CCN population. Model coefficients N_0 and P in a power law function of water supersaturation (SSW) for the CCN activity $N (\text{cm}^{-3})$ ($N = N_0 \text{SSW}^P$) were adjusted to agree with the experimentally observed droplet concentrations that actually nucleated at the different updraft rates. Also, ice nucleation was adjusted to be as equivalent as possible to the experiments at the onset of cloud. Supersaturation is diagnosed in the model, so the choices of N_0 and P that agreed with droplet concentrations nucleated also determined the peak supersaturation value in each case. For N_0 on the order of the number of soot particles injected into the chamber, the choice of P is not very important. A value of 1.0 was chosen. The major contribution to the uncertainty in the estimation of SSW is the uncertainty in actual droplet concentrations nucleated. As discussed by DeMott and Rogers (1990), there are few factors which could contribute to the FSSP concentration uncertainty with the sample system employed. However, they noted record to record variations of as much as 30% in FSSP concentrations, which may reflect true inhomogeneities in the clouds formed. This was also evident in this study, and is considered in determining the uncertainty of model estimated SSW.

3. Results

Time, temperature, cloud properties (droplet concentration and average diameter) and the cumulative number of ice crystals formed in the chamber volume in one experiment are plotted versus pressure in Fig. 3. Simulated ascent rate was 5 m s^{-1} in this experiment. Cooling rate was approximately 3°C min^{-1} until cloud formed and 2°C min^{-1} thereafter. Droplet dispersion values about the mean were approximately 0.2 to 0.3, with sizes ranging from 1 to 15 μm . Cloud water was depleted due to overwhelming competition from ice crystal growth at the coldest temperatures. It is tempting to infer that the apparent increase in droplet concentrations later in the experiment are a result of droplet measurement interference due to ice crystals, but this feature is within the uncertainty of droplet measurements, and little coincident increase in particle size is noted (as might be expected). In any case, the response of the FSSP to ice crystals is not well known, and any interference would occur at the point of total cloud glaciation, after the experimental period in which ice nucleation rates were evaluated in this study.

Figure 4 shows the fraction (of the total number present) of 0.08 μm soot particles activated as cloud droplets, and the instantaneous (s^{-1}) and cumulative soot fractions which nucleated ice crystals, as a function of temperature in the 5 m s^{-1} simulated ascent. Essentially all (93%) of the soot acted as CCN, based on FSSP concentration values averaged over the first 5 minutes after cloud formed. Peak supersaturation was estimated by the adiabatic cloud model as $2.0 \pm 0.3\%$

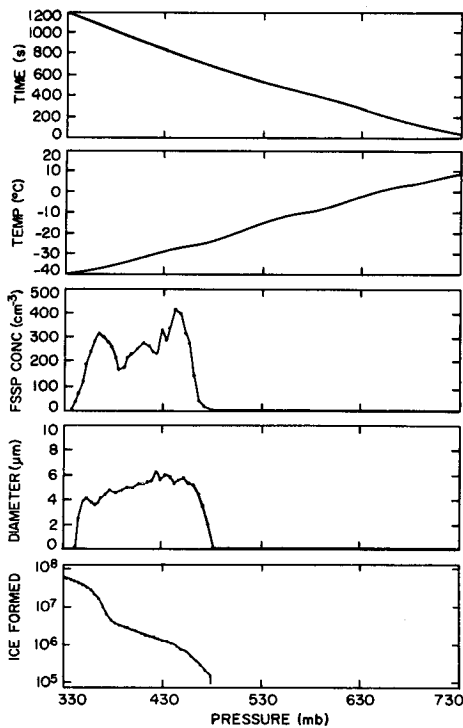


FIG. 3. Time, temperature, cloud quantities, and cumulative ice crystal numbers formed versus pressure during a simulation of a 5 m s⁻¹ adiabatic ascent of an air parcel containing soot aerosol. Data are taken at 15 s intervals. Cloud droplet concentration and average diameter (measured with FSSP) are 15 s average values. Note the experiment proceeds from higher to lower pressure (right to left).

in this case. There was some evidence of ice formation by deposition (before cloud formed), although the experimental method is not really appropriate to the identification of deposition which occurs very close to cloud point. Certainly, ice did not precede cloud by much in this experiment. Some condensation-freezing nucleation may have occurred at cloud point (-23.7°C), but moderate nucleation continued until -34°C, most likely indicating immersion-freezing. Very strong ice nucleation occurred colder than -34°C, and this feature is interpreted as primarily homogeneous-freezing nucleation since it is very similar to other experiments with soluble salt CCN. More will be said about this feature later.

In the 2.5 m s⁻¹ simulated ascent with 0.08 μm soot particles injected, peak estimated supersaturation was

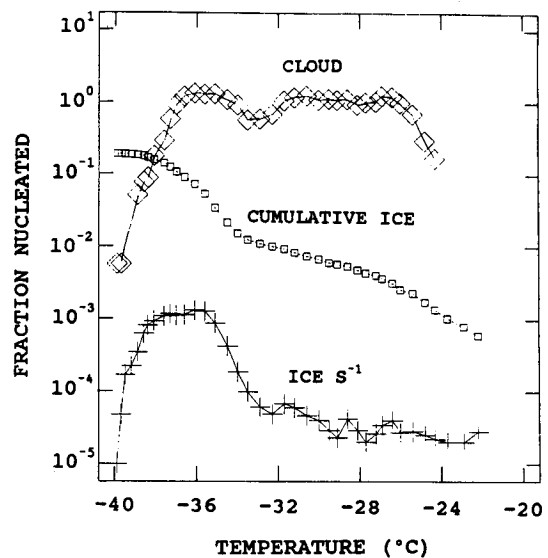


FIG. 4. Fractions of 0.08 μm soot nucleated as water and as ice with respect to the total soot aerosol number initially present during the same expansion test shown in Fig. 2.

1.4 ± 0.2% and only about 58% of the aerosols formed cloud droplets (see Table 1). This result is in reasonable agreement with CCN active fractions between 0.2 and 0.5 for acetylene (at 1% water supersaturation) reported by Hallett et al. (1989). Particles not activated as CCN were available for form ice by modes other than condensation-freezing and immersion-freezing. However, Table 1 shows that the percentage fraction of ice nucleating aerosol was about 50 to 70% of that in the faster ascent rate experiment. Hence, the ice nucleating activity appears to primarily occur by way of immersion-freezing. This is emphasized in Fig. 5, where ice nucleating fractions are displayed after computation with respect to the fractions immersed in cloud droplets at any point during cooling. Exemplary uncertainties, which increase in magnitude with the fraction nucleated, are also displayed. These are based on a standard error analysis that includes stated uncertainties in temperature, ice particle detection, and droplet concentration. The cumulative numbers of the aerosols freezing with respect to the numbers immersed in cloud droplets are essentially independent of cooling rate for the 0.08 μm particles. This is expected for "like" ice nuclei distributed one per drop.

TABLE 1. Summary of soot as CCN and immersion-freezing nuclei.

Size (μm)	dT/dt (°C min ⁻¹)	SSW (%) (est.)	[Drops]/[CN]	Cumulative fraction nucleated at T (°C)					
				(-24)	(-26)	(-28)	(-30)	(-32)	(-34)
.08	1.1	1.4 ± 0.2	0.58	0.0006	0.0017	0.0026	0.0042	0.0061	0.0089
.08	2.0	2.0 ± 0.3	0.93	0.0012	0.0026	0.0047	0.0068	0.0098	0.0154
.12	1.1	1.4 ± 0.2	0.62	0.0014	0.0034	0.0059	0.0078	0.0105	0.0132

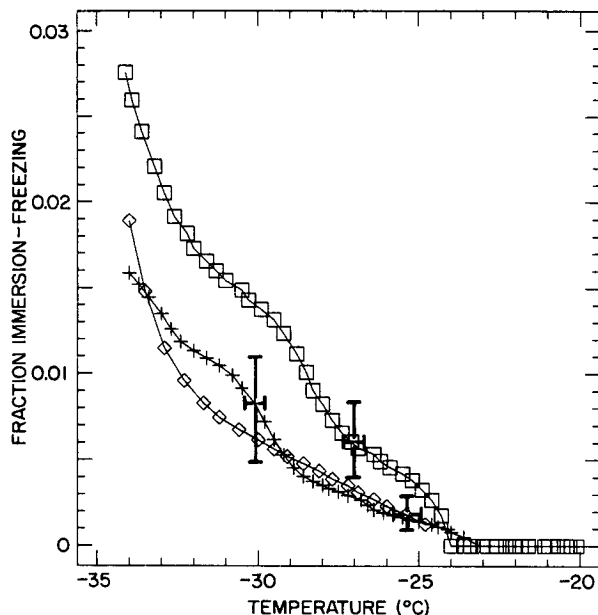


FIG. 5. Fractions of soot nucleated as ice with respect to the numbers of aerosol immersed in cloud droplets for $0.08\ \mu\text{m}$ soot in $1^\circ\text{C}\ \text{min}^{-1}$ ($+\text{---}$) and $2^\circ\text{C}\ \text{min}^{-1}$ ($-\diamond-$) cooling rate expansions, and for $0.12\ \mu\text{m}$ (actual diameter, not mobility diameter) soot in $1^\circ\text{C}\ \text{min}^{-1}$ cooling rate expansion ($-\square-$). Uncertainties are noted by horizontal and vertical bars at one data point in each experiment.

For the larger aerosol ($0.15\ \mu\text{m}$ mobility diameter), Table 1 shows that for the same cooling rate, slightly higher fractions of $0.15\ \mu\text{m}$ soot nucleated as CCN compared to $0.08\ \mu\text{m}$ soot. Fractions of $0.15\ \mu\text{m}$ soot which nucleated ice were significantly higher. Since contact-freezing nucleation would be very limited for these larger particles, the increase is due to additional activity as deposition nuclei or to a more efficient immersion-freezing process for the larger particles. The activity is presented as immersion-freezing activity in Fig. 5, for comparison to the $0.08\ \mu\text{m}$ soot data. The increased activity of the larger particles is in qualitative agreement with thermodynamic theory for immersion-freezing nucleation (i.e., Fletcher 1959) which predicts that nucleation rate should increase as the square of the radius. In this case, the rate theoretically should increase by 3.5, based on electrical mobility diameters. A factor of about 2.0 was observed across the -24° to -34°C temperature range, in very good agreement with the fact that the actual diameter of the larger soot particles was about 20% less than the mobility diameter, or $0.12\ \mu\text{m}$.

Accepting the hypothesis of immersion-freezing as the dominant nucleation mode responsible for ice formation of these experiments, it is possible to fit a power law versus temperature to the data of the form,

$$F = 4\pi r_p^2 A (\Delta T_s)^B \quad (1)$$

where F is the fraction freezing of the number individually immersed in activated cloud droplets, r_p is the

soot particle radius, ΔT_s is supercooling, and A and B are constant coefficients. This equation, with $A = 1.002 \times 10^4$ and $B = 7.767$, is consistent with 96% of the variance for all of the data presented in Figure 5 considered as one sample. Predicted active site densities (sites cm^{-2}) are about 10^6 at -20°C and 10^8 at -36°C . Equation (1) is strictly valid from about -22° to -34°C .

Tests have not been made to establish any time dependence of nucleation at a single temperature. The results of Vali and Stansbury (1966) suggest that this is a secondary effect, although Baldwin and Vonnegut (1984) show a distinct stochastic effect for silver iodide in bulk water for the several degrees below its threshold nucleation temperature. If time dependence were a significant factor in these experiments, then the slower cooling rate test would have higher relative fractions nucleated. This does not agree with the experimental results presented. Certainly more tests are needed to establish statistical significance and to isolate the contributions of contact-freezing and deposition.

It may be noted that in all tests, nucleation rate increased sharply below about -34°C , eventually causing total cloud glaciation. The nucleation response at the coldest temperatures was similar to that observed during the freezing of relatively pure cloud droplets formed on soluble CCN in this same chamber (DeMott and Rogers, 1990). The freezing rate per unit volume J_{1s} ($\text{cm}^{-3}\ \text{s}^{-1}$) of those dilute solution droplets was interpreted to represent homogeneous-freezing nucleation rates. This provides a plausible explanation of the increased ice nucleation below -34°C . Essentially disregarding the fact that every drop contained a potential heterogeneous ice nucleating particle in the three soot experiments, J_{1s} values were calculated here. They are presented in Fig. 6 for comparison with the average rates obtained for cloud droplets formed on soluble CCN. The calculation procedure follows DeMott and Rogers, and uses the mean volume droplet diameter to characterize the droplet size distribution. The solid line shows the regression of the data in DeMott and Rogers; it explains 74% of the variance of their data. The dashed lines represent the uncertainty associated with the mean values. The uncertainty in the J_{1s} calculations made for the soot experiments is the same. The freezing rate per unit volume calculated for the soot experiments is nearly constant ($\sim 6 \times 10^5$) between -26° and -34°C , but increases by three orders of magnitude from -34° to -39°C . Below about -34°C , J_{1s} falls within the envelope of J_{1s} for soluble CCN experiments. Nucleation of ice is clearly heterogeneous above -34°C , but is probably spontaneous at colder temperatures.

4. Summary

Exploratory experiments were performed to study some aspects of the ice nucleating behavior of freely suspended carbonaceous soot aerosols in laboratory-

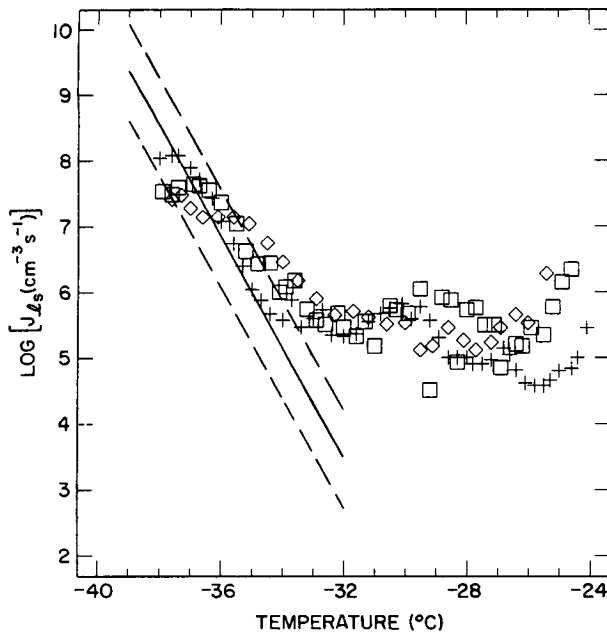


FIG. 6. Computations of homogeneous-freezing nucleation rate ($\text{cm}^{-3} \text{s}^{-1}$) for the cloud droplets present in the three soot aerosol experiments, disregarding the effect of the heterogeneous particles. Different symbols denote the different experiments. Results of computations are compared to the freezing nucleation rates for droplets formed on soluble CCN, represented by the solid line (with dashed line uncertainties) from DeMott and Rogers (1989).

simulated natural clouds at temperatures colder than -20°C . The CCN activity of the soot aerosols generated was used to encapsulate a large proportion of the aerosols in cloud droplets during expansional cooling. Experiments indicate an increase in fractional CCN activity versus particle size and with supersaturation. Equivalent simulations with a numerical cloud model were used to estimate that all of the soot would act as CCN as water supersaturations approach 2%. The value of this threshold probably varies with specific soot chemistry. More rigorous studies of CCN activity versus supersaturation are needed to make the results of this study most relevant to atmospheric conditions. Immersion-freezing nucleation is a particularly efficient ice nucleation mode after water has condensed on soot.

Ice formation attributed to immersion-freezing was found to be directly proportional to the soot fraction immersed in droplets, and to the particle area. A combination of (1) with a rigorous measure of CCN activity versus particle size, should permit the prediction of ice formation by this mechanism under a wide range of atmospheric conditions. At colder temperatures, the immersion-freezing mechanism is superseded by homogeneous-freezing nucleation. This transition will depend on the droplet size. In the present experiments, this occurred below -34°C .

If one takes the standard definition of the "threshold temperature" for ice formation as 1 particle in 10^4

producing an ice crystal, then this temperature (assuming all particles are immersed in drops) can be predicted from (1) as -17.7°C for $0.08 \mu\text{m}$ diameter soot, and -16°C for $0.12 \mu\text{m}$ diameter soot. The threshold temperatures of most particles thought to be responsible for natural ice formation in the atmosphere (i.e., clay particles of surface soil origin) range from -4° to -20°C , depending on the material and the nucleation mode. Hoffer (1961) found immersion-freezing thresholds for both kaolinite and montmorillonite, two known ice nucleating materials, to be -13.5°C . Pitter and Pruppacher (1973) gave the immersion-freezing threshold for these same materials as -14°C . These thresholds are only a few degrees warmer than for the soot tested in this study. However, the studies by Hoffer and by Pitter and Pruppacher noted complete activation by immersion-freezing at temperatures between -24° and -32°C . This contrasts with the results for soot presented in this paper, where only 1.5% to 3% of the particles nucleated freezing in supercooled drops after cooling to -34°C . A basic experimental difference between this study and the earlier studies noted was the assurance in the present study that each droplet contained only one potential ice nucleus. Still, the basic conclusion is that the typical soil particles in air are a much more plentiful and active source of ice nucleating aerosols than the source from soot particles, except in situations which lack soil particles or in which soot is present in excessive concentrations.

Results of the type presented in this paper represent only one component of a complete description of nucleation by soot in the atmosphere. For example, for conditions in cirrus clouds, where water supersaturations may only exist for transient periods and may only be a few tenths of a percent, the immersion-freezing contribution to ice formation would be much smaller. In such cases, other nucleation modes might act at competitive rates. The noted direct relationship between the magnitude of ice formation and the immersed soot fraction in the experiments reported, suggests that other ice formation mechanisms may be of minor importance. In that case, the results presented are descriptive of the main component of the ice nucleation scavenging characteristics of carbonaceous soot. Further studies are needed to verify these preliminary experiments, to examine the effect of such factors as evaporation and recondensation on immersion-freezing activity, and to specifically isolate the contributions, if any, of other ice nucleation modes.

Acknowledgments. This research was sponsored by the National Science Foundation Grants ATM-8813345, ATM-8704776 and ATM-8519370, and USAF Contract F336567-86-C-3002. I would like to thank Professor Lewis O. Grant and Dr. David C. Rogers for their helpful comments and assistance in this research. Special thanks to Lucy McCall for drafting the figures.

REFERENCES

- Baldwin, and Vonnegut, 1984: Repeated nucleation of a supercooled water sample that contains silver iodide particles. *J. Climate Appl. Meteor.*, **23**, 486–490.
- Baumgardner, D., W. Strapp and J. E. Dye, 1985: Evaluation of the forward scattering spectrometer probe. Part II: Corrections for coincidence and dead-time losses. *J. Atmos. Oceanic Technol.*, **2**, 636–643.
- Cleary, T., G. Mulholland and J. W. Gentry, 1988: The experimental measurements of clusters formed from soot near the sooting limit. Atmospheric Aerosols and Nucleation, *Proc. of the 12th Int. Conf. on Atmospheric Aerosols and Nucleation*, P. Wagner and G. Vali, Eds., Lecture Notes in Physics, No. 309, Springer Verlag, 120–123.
- Cooper, W. A., 1988: Effects of coincidence on measurements with a Forward Scattering Spectrometer Probe. *J. Atmos. Oceanic Technol.*, **5**, 823–832.
- DeMott, P. J., 1988: Comparisons of the behavior of AgI-type ice nucleating aerosols in laboratory-simulated clouds. *J. Wea. Mod.*, **20**, 44–50.
- , and D. C. Rogers, 1990: Freezing nucleation rates of dilute solution droplets between -30 and -40°C in laboratory simulations of natural clouds. *J. Atmos. Sci.*, **47**, 1056–1064.
- Dye, J. E., and D. Baumgardner, 1985: Evaluation of the Forward Scattering Spectrometer Probe. Part I: Electronic and optical studies. *J. Atmos. Oceanic Technol.*, **1**, 329–344.
- Fletcher, N. H., 1959: On ice crystal production by aerosol particles. *J. Meteor.*, **16**, 173–180.
- Hagen, D. E., M. B. Trueblood and D. R. White, 1989: Hydration properties of combustion aerosols. *Aerosol. Sci. Technol.*, **10**, 63–69.
- Hallett, J., B. Gardiner, J. Hudson and F. Rogers, 1986: Cloud condensation and ice nucleation of a range of carbonaceous aerosols. Preprints, *Amer. Meteor. Soc. Conf. on Cloud Physics, Vol. 2*, Snowmass, Amer. Meteor. Soc., 9–12.
- , J. Hudson and F. Rogers, 1989: Characterization of combustion aerosols for haze and cloud formation. *Aerosol. Sci. Technol.*, **10**, 63–69.
- Hoffer, T., 1961: A laboratory investigation of droplet freezing. *J. Meteor.*, **18**, 766–778.
- National Research Council, *The Effects on the Atmosphere of a Major Nuclear Exchange*. National Academy Press.
- Pinnick, R. G., and H. J. Auvermann, 1979: Response characteristics of Knollenberg light-scattering aerosol counters. *J. Aerosol Sci.*, **10**, 55–74.
- Pitter, R., and H. Pruppacher, 1973: A wind tunnel investigation of freezing of small water drops falling at terminal velocity in air. *Quart. J. Roy. Meteor. Soc.*, **99**, 540–550.
- Pruppacher, H. R., and M. Neiburger, 1963: The effect of water soluble substances on the supercooling of water drops. *J. Atmos. Sci.*, **20**, 376–385.
- Sinclair, D., 1986: Measurement of nanometer aerosols. *Aerosol. Sci. Technol.*, **5**, 187–204.
- Vali, G., 1985: Nucleation terminology. *J. Aerosol Sci.*, **16**, 575–576.
- , and E. J. Stansbury, 1966: Time-dependent characteristics of the heterogeneous nucleation of ice. *Can J. Phys.*, **44**, 477–502.
- Young, K. C., 1974: A numerical simulation of wintertime orographic precipitation: Part I. Description of model microphysics and numerical techniques. *J. Atmos. Sci.*, **31**, 1735–1748.
- , 1977: A microphysical parcel model. 1974–Revised 20 January 1977. University of Arizona, Tuscon, 67 pp.